Earth Syst. Dynam. Discuss., 6, 2507–2542, 2015
www.earth-syst-dynam-discuss.net/6/2507/2015/
doi:10.5194/esdd-6-2507-2015

Earth System Dynamics
Discussions
Open Access

Early warning signals in complex ecosystems

I. S. Weaver and J. G. Dyke

School of Geography and Environment, University of Southampton, University Road, Southampton, SO17 1BJ, UK

Received: 8 October 2015 – Accepted: 23 October 2015 – Published: 27 November 2015

Correspondence to: I. S. Weaver (isw1g10@soton.ac.uk)

Published by Copernicus Publications on behalf of the European Geosciences Union.

Abstract

Given the potential for elements of the Earth system to undergo rapid, hard to reverse changes in state, there is a pressing need to establish robust methods to produce early warning signals of such events. Here we present a conceptual ecosystem model in which a diversity of stable states emerge, along with rapid changes, referred to as critical transitions, as a consequence of external driving and non-linear ecological dynamics. We are able to produce robust early warning signals that precede critical transitions. However, we show that there is no correlation between the magnitude of the signal and magnitude or reversibility of any individual critical transition. We discuss these findings in the context of ecosystem management prior to and post critical transitions. We argue that an understanding of the dynamics of the systems is necessary both for management prior and post critical transitions and the effective interpretation of any early warning signal that may be produced for that system.

1 Introduction

It has been proposed that many elements of the Earth system could exhibit critical transitions; abrupt changes to the state of a system caused by perturbations, marking the onset of a new, long-term regime (Scheffer et al., 2009). Critical transitions are properties of multi-stable systems and are described mathematically via catastrophic bifurcation theory (Zeeman, 1976). They are ubiquitous across a diversity of microscopically distinct systems; including ecological, socio-economic and climate systems (Scheffer et al., 2001; May et al., 2008; Lenton et al., 2012). Furthermore they occur over a wide range of spatial and temporal scales: days and meters for lake systems undergoing a transition from clear water, macrophyte dominated to turbid water, algae dominated (Carpenter et al., 1999); years and kilometres for forest die back and deforestation (van Nes et al., 2012); centuries and global scale for climate dynamics (Lenton et al., 2008). Given concerns over anthropogenic impacts on the

Earth system, assessing a system's propensity to undergo a critical transition has become a subject of intense research (Scheffer et al., 2015). There are also attempts to predict critical transitions at some point before their onset. For example critical slowing-down refers to the long relaxation time of near-critical systems, those which are approaching climatic or ecosystem transitions (Scheffer et al., 2009; Lenton, 2011), while it has been shown that certain time series find an increase in the auto-correlation coefficient precedes such transitions (Dakos et al., 2008).

In order to progress the analysis of critical transitions and associated early warning signals in Earth system processes we aim to produce a minimal model of the feedback between Earth's biota and the abiotic environment. We emphasise tractability, in the sense that we are able to draw generalities where behaviour emerges from principle model assumptions rather than our specific implementation, without shying away from the complexity which emerges from non-linear systems with multiple environmental dimensions. From key assumptions, the simple model produces multiple homeostatic attractors, proving robust to external perturbations (Dyke and Weaver, 2013). The complex behaviour of the model belies its broad tractability which we utilise to derive a number of analytical results. We determine the distribution both of stationary points and critical transitions encountered by increasing or decreasing external forcing terms analytically, going on to analyse the behaviour of the model in the vicinity of stable fixed points, particularly how this behaviour changes as the system approaches a transition. In doing so we generate early warning signals of impending critical transitions. These early warning signals do not give any information about the magnitude of the critical transition, nor to what extent the transition may be irreversible. We discuss these results in the light of conceptual and empirical studies on complex Earth system processes and possible critical transitions.

2 Critical transitions in the Earth system

Critical transitions, regime shifts or tipping points have been shown in a number of biophysical, socio-economic and psychological processes (Scheffer et al., 2001; May et al., 2008; Venegas et al., 2005). These systems appear to share only their high degree of connectivity, diversity and complexity in common from which critical transitions emerge as a general property. Systems approaching a critical point are at the cusp of a significant transition where noise or very minor adjustments to perturbing forces can tip the system from one state to another; we say its susceptibility to these changes diverges and in practice, a stochastically perturbed system would see an increasing variance in its state variables (Carpenter and Brock, 2006). In addition to large susceptibility, the near-critical dynamics of such systems are slow such that fluctuations which do not cause transitions are reigned back to the steady-state very weakly. This is referred to as an increasing decay time, or as a decreasing recovery rate. As before, the signal produced from a slow system would be detectable, but this time rather than increasing variance, one would detect trends over longer time scales due to slower relaxation (Kleinen et al., 2003). These phenomena are both symptoms of critical slowing down; a term which originates from physics in the context of phase transitions but is no different in the Earth-system context.

A mechanism for CSD is proposed by Scheffer et al. (2001); the potential well associated with the current state flattens as a transition is approached, illustrated by Fig. 1. Forces which restrain the system to a fixed point are determined by the gradient of the potential, $\nabla\phi$, and so a flattening of the potential corresponds to weaker restraints and therefore larger, slower fluctuations about the stationary state. Another consequence of the illustration is a reduction in the potential wall which separates the current state from the state it will transition into, resulting in asymmetry of the potential. Guttal and Jayaprakash (2008) suggest that along with the increasing variance and autocorrelation, a signal may reflect this asymmetry through increasing skewness; fluctuations about the mean signal will have different sizes in different directions, particularly the direction of the transition. Long relaxation times and skewness have been found in a range of climatic and ecosystem transitions; perhaps most famously, the last transition to the present icehouse state from a hot greenhouse state with no continental glaciation was precursed by a slowing in the variability of surface temperatures, estimated from the composition of ocean sediment. Within this icehouse state are further transitions between interglacial and glacial states, associated with the retreat or growth of ice sheets. These transitions are accompanied by similar signals in the ice core deuterium record, a proxy for the Antarctic temperatures (Scheffer et al., 2009; Lenton, 2011; Sornette, 2002). These methods have recently been adopted to evaluate ecosystem stability where transitions in trophic structure have been found to be accompanied by CSD in certain population dynamics (Carpenter et al., 2011).

In this study, we focus on critical transitions that feature important biological processes. Initially, critical transitions or tipping points in the Earth system as a consequence of anthropogenic climate change is within this set as a particular species – Homo sapiens – is driving the climate via emissions of greenhouse gasses and land use change. We further refine the set by requiring that the critical transition itself is in part a consequence of biological effects. A classic example is lake eutrophication in which the transition to turbid, reduced biodiversity state in response to progressive inputs of phosphorus and/or nitrogen fertilisers comes as a consequence of the bloom of large algae populations which drives bottom water anoxia and so promotes leaching of phosphorus sequestered in sediments back into the lake water (Carpenter, 2005). In the clear water state, limiting nutrients are often kept at very low levels via the process of “biotic plunder” (Tyrrell, 2004). Progressively higher input of phosphorus is able to tip the system into a period of positive feedback and rapid transition from one attractor to another. Models such as Carpenter et al. (1999) capture these types of dynamics although they do so by empirically parameterising certain non-linear functions.

In many respects, it is appreciated that these simple hysteresis loops which occur in systems of one control dimension are a useful allegory for the behaviour of very much more complicated systems, of which almost all real systems may be considered an example. However there is a relative paucity of research which extends such iconic phenomena to more complicated, high dimensional systems. Establishing a simple and tractable model, which retains the high dimensionality and complexity that underpins real Earth systems is our central motivation, formulated from key assumptions in the following section.

3 Model formulation

The model formulation can be summarised as a non-linear feedback loop between environmental and biotic elements; the environment determines the steady-state composition of the biota through a non-linear function. In turn, key environmental variables are effected by contributions both from the biota, and external perturbations, such as from anthropogenic sources, parametrised by a linear function. Along with the core mechanism, the biota and environment operate their own internal feedback mechanisms, a system illustrated by Fig. 2, and explained in detail in this section. The model builds upon previous work (Weaver and Dyke, 2012; Dyke and Weaver, 2013; Weaver and Dyke, 2013), extending the model with the inclusion of feedback mechanisms within the biotic and environmental components, not just between them. In doing so, we further extend the generality of the model without sacrificing any of the appealing tractability.

The biota is represented by a large number, K, of independent and randomly parametrised biotic elements. Rather than imposing any assumptions about the form the biota takes, their individual abundance, metabolic activity or overall influence is denoted by the positive vector $\boldsymbol{\alpha}$. These elements interact with a simple environment, comprised of N key environmental variables denoted by the vector $\boldsymbol{E}$. The effect of individual biotic elements is unidirectional and monotonic; each species has only an increasing or decreasing effect on each aspect of the environment which is directly proportional to their biotic activity. These minimal ingredients, encapsulated in Fig. 2, have been shown to produce a range of ecological dynamics (Dyke and Weaver, 2013). Most significantly, homeostatic fixed points in the environmental variables emerge over a wide range of assumptions merely from the effects of a randomly assembled biota.

i. Environment affects life

Each element of the biota has an optimal environment which we refer to as its niche; a point in the space of environmental variables where its activity is maximised. The time evolution of each element of the biota is a relaxation towards some steady-state activity $\boldsymbol{\alpha}^*$ with characteristic time scale τ_α and according to some function.

$$\tau_\alpha \frac{\mathrm{d}\boldsymbol{\alpha}(t)}{\mathrm{d}t} = f\left(\boldsymbol{\alpha}(t), \boldsymbol{\alpha}^*(\boldsymbol{E}, \boldsymbol{\mu})\right) \tag{1}$$

where $\boldsymbol{\alpha}^*$ is the fixed point in the time evolution of $\boldsymbol{\alpha}$, dictated by the state of the environment and a niche parameter unique to the each biotic element $\boldsymbol{\mu}$, and f is some function which stable root at $\boldsymbol{\alpha}$, its fixed point value. The simplest choice would be a linear relaxation which can be used as an approximation of other non-linear functions providing the biota is in the vicinity of its fixed point where $\boldsymbol{\alpha}^*(\boldsymbol{E}, \boldsymbol{\mu}) - \boldsymbol{\alpha}(t)$ is small;

$$f\left(\boldsymbol{\alpha}(t), \boldsymbol{\alpha}^*(\boldsymbol{E}, \boldsymbol{\mu})\right) = \boldsymbol{\alpha}^*(\boldsymbol{E}, \boldsymbol{\mu}) - \boldsymbol{\alpha}(t). \tag{2}$$

Activity is maximised at $\boldsymbol{\mu}$ and decays by some function as the environment departs the niche. Niches are randomly distributed uniformly in a finite volume of environmental variables called the essential range, which imposes limits on the ability of the biota to prosper in extreme environmental conditions. For simplicity, it is equal in all environmental variables and denoted σ_μ. Providing a sufficiently large biota which densely populates the essential range, the exact choice of $\boldsymbol{\alpha}^*$ can be shown to be arbitrary (Dyke and Weaver, 2013), although we choose a Bell-curve in the N environmental dimensions for visualisation;

$$\alpha_i^*(\boldsymbol{E},\boldsymbol{\mu}) = \exp\left(-\frac{|\boldsymbol{\mu}_i - \boldsymbol{E}|^2}{2\sigma_E^2}\right) \tag{3}$$

where σ_E is the niche width.

ii. Life affects environment

The persistence of life requires some influence on the local environment, at the very least through the chemical processes involved in metabolism, although organisms may have further effects on abiotic factors, either directly or through their influence on other abiotic processes such as weathering. Modifications to the local environment by organisms is encapsulated by concepts of niche construction and ecosystems engineering (Jones et al., 1994; Odling-Smee et al., 2003), and occur over a range of spatial and temporal scales; from changes in soil composition to that of the atmosphere globally (Wilkinson et al., 2009; Sanders and van Veen, 2011; Goldblatt et al., 2006).

Rather than resolving particular biological processes, the simplest implementation of biotic effects is to assign each element a positive or negative influence on each environmental variable which increases in magnitude linearly with the biotic activity. This is achieved by populating the matrix $\boldsymbol{\Omega}$ with independent random variables, where the cumulate effect of the biota on each environmental variable, $\boldsymbol{F}$ is be found from the matrix product

$$\boldsymbol{F}(t) = \boldsymbol{\Omega}\cdot\boldsymbol{\alpha}(t). \tag{4}$$

The effects in $\boldsymbol{\Omega}$ are chosen randomly from the standard normal distribution, where the mean value of zero provides no bias towards positive or negative life-environment coupling. The steady-state effect of two opposing biotic elements on one environmental variable are shown by Fig. 3a, while the cumulative effect of a diverse biota is shown by Fig. 3b.

The environmental variables are linearly driven by contributions from the biota $\boldsymbol{F}$ and external abiotic influences $\boldsymbol{P}$. That is to say, in the presence of even weak forcing we do not assume any fixed-point within the essential range to exist, and the environmental conditions will monotonically depart the essential range.

$$\tau_E \frac{\mathrm{d}\boldsymbol{E}(t)}{\mathrm{d}t} = \boldsymbol{F}(t) + \boldsymbol{P}(t). \tag{5}$$

The linear time evolution of $\boldsymbol{\alpha}$ ensures this system has a $2N$-dimensional phase space (Weaver and Dyke, 2013) though this can be reduced to N-dimensions if the time scales of processes associated with changes in the biota, $\boldsymbol{\alpha}$ and the environment, $\boldsymbol{E}$ may be assumed separated, such that changes to the ecology occur on very much shorter time scales than those to the environment, or $\tau_\alpha \ll \tau_E$. In this instance, the activity of the biota may be replaced by its steady-state value $\boldsymbol{\alpha}^*$ and the model is reduced to a single equation

$$\frac{\mathrm{d}\boldsymbol{E}(t)}{\mathrm{d}t} = \boldsymbol{\Omega} \cdot \boldsymbol{\alpha}^*(\boldsymbol{E}, \boldsymbol{\mu}) + \boldsymbol{P}(t). \tag{6}$$

It is useful to ensure that important model characteristics are invariant with the arbitrary model parameters, those which are neither random nor fundamental model components. This enables direct comparison of model behaviour over a range of parameters which might otherwise be obfuscated. We rescale the effect of the biota by introducing the normalisation constant

$$(\boldsymbol{\Omega} \cdot \boldsymbol{\alpha}) \rightarrow C^{-1}(\boldsymbol{\Omega} \cdot \boldsymbol{\alpha}) \tag{7}$$

where we have used the constant C to normalize the total biotic effect, $\boldsymbol{F}(\boldsymbol{E})$ such that its variance is independent of the fundamental niche width, σ_μ, and the number of biotic components, K.

$$C^2 = \sqrt{\pi} K \frac{\sigma_E}{\sigma_\mu}. \tag{8}$$

These two model aspects are all that is required for multiple stable states and homeostatic behaviour. In the following sections we provide simple mechanisms to govern feedback both within the biota and its environment to prove that such additional details do not undermine salient model behaviour, explored by Dyke and Weaver (2013).

iii. Including interactions within the biota
Individuals, populations and species will interact with others via a range of ecological processes. These may be trophic in the form of predator prey relationships, or competitive exclusion from shared resources. Here we implement these biotic interactions via a series of Lotka-Volterra equations. We populate a matrix, **C**, from an arbitrary zero-mean distribution with unit variance, such as the standard normal distribution. These elements provide increases or decreases the activity of each biotic element in proportion to their own activity by the competitive Lotka-Volterra equation. Intraspecific interactions are governed by our choice of $\boldsymbol{\alpha}^*$ such that in the absence of further interspecific interactions (if **C** is the identity matrix), populations will approach $\boldsymbol{\alpha}^*(\boldsymbol{E},\boldsymbol{\mu})$ exactly as with the non-interacting biota. The time evolution of the coupled biota is

$$\tau_\alpha \frac{\mathrm{d}\alpha_i}{\mathrm{d}t} = \alpha_i \left(1 - \frac{\sum_{i=1}^{K} c_{i,j}\alpha_j}{\alpha^*(\boldsymbol{E},\boldsymbol{\mu}_i)}\right) \tag{9}$$

which has a number of trivial fixed points where either all populations are extinct $\alpha_i = 0\ \forall_i$ or where single population exists $\alpha_i = \alpha{*}_i$ with all others being extinct $\alpha_i = 0 \forall_i \neq j$. However for all weakly diagonally dominant coupling matrices we attain a globally attractive non-trivial solution where there is significant contribution from a finite proportion of the biota (Lu, 1998).

To see the influence of the competitive mechanism on the composition of the biota, we can directly compare it to that which would be produced by a non-interacting biota. The new mechanism does not compromise the diversity of biotic elements any more than our defined niche width does, illustrated by the correlations in the effect function $\boldsymbol{F}$ with changes in the environment $\boldsymbol{E}$, shown for one environmental dimension in Fig. 4. Note that we do not allow any elements of the biota to become extinct; they are able to re-emerge from negligible activity if the environment shifts favourably. Here we see that the characteristic length scale of the effect function is maintained although the complex behaviour of our K-dimensional competitive Lotka-Volterra equation introduces finer scale effects which are expected to vanish in the limit of large K.

iv. Including abiotic feedback

Previously we have assumed no dynamics besides those generated by the shifting composition of the biota; abiotic perturbing forces drive the environment uniformly within the essential range. The model can be modified to incorporate feedback systems within the environment which can be seen as an abiotic perturbation which varies in $\boldsymbol{E}$. This may draw abiotic systems into a fixed point, or repel them from one depending on the properties of the coupling matrix $\mathbf{D}$ which may induce positive or negative environmental feedback. We parametrise the relative importance of biotic and abiotic processes with a scalar, φ,

$$\frac{\mathrm{d}\boldsymbol{E}(t)}{\mathrm{d}t} = \boldsymbol{\Omega} \cdot \boldsymbol{\alpha}^{*}(\boldsymbol{E},\boldsymbol{\mu}) + \varphi \mathbf{D}\left(\boldsymbol{E}^{*} - \boldsymbol{E}\right). \tag{10}$$

As a simple example, we design a two-dimensional system with two coupling matrices which, in the absence of the biota, lead to positive and negative feedback, labelled $\mathbf{D}_{\text{pos.}}$ and $\mathbf{D}_{\text{neg.}}$ respectively.

$$\mathbf{D}_{\text{pos.}} = \begin{pmatrix} 1 & 0 \\ 0 & 1 \end{pmatrix}, \qquad \mathbf{D}_{\text{neg.}} = \begin{pmatrix} 0 & -1 \\ -1 & 0 \end{pmatrix}. \tag{11}$$

We can observe the influence of these mechanisms along with a diverse biota in Fig. 5 for a range of φ, although the result may also be intuited from previous work.

The definition Eq. (10) ensures that the feedback term increases in magnitude with the distance from the fixed point $\boldsymbol{E}^*$. We have found the magnitude of the biotic effect to be normally distributed, and therefore configurations which oppose large forces are rare, and the density of fixed points decreases as we depart $\boldsymbol{E}^*$. $\mathbf{D}_{\text{neg.}}$ constrains the system by the increasing attraction of $\boldsymbol{E}^*$ which, in the limit of large φ, becomes absorbing. On the other hand, $\mathbf{D}_{\text{pos.}}$ repels the system, eliminating fixed points in the essential range, as indicated by the white regions of Fig. 5.

4 Emergence of critical transitions

In summary, the model produces a number of biotically mediated homeostatic fixed points within the essential range of environmental variables, even in the face of external perturbations or destabilising environmental feedback. The number density of these points decreases with the magnitude of perturbing forces as expected, and variation of forcing strength creates a network of hysteretic states between them, including the emergence of cusp bifurcations, where the nature of a transition encountered by variations in one forcing dimension depends on other forcing dimensions. Both the density of homeostatic states and critical transitions may be derived analytically. This section details these key results.

For all figures, the essential range is fixed at $\sigma_\mu = 100$ within which the niches of individual biotic elements are distributed uniformly. Previous work has illustrated that beyond a threshold, further increases in the diversity of the biota, K do not significantly alter the behaviour of the model and the biotic effect function $\boldsymbol{F}$ is well approximated by a Gaussian process which shares the covariance of individual niche functions (Dyke and Weaver, 2013). The expected number of fixed points within the essential range is instead determined by the characteristic width of the niche function which we set as $\sigma_E^2 = 50$ as a compromise between diverse attractor structures and ease of interpretation. Similarly, we choose a model of $N = 2$ environmental variables as the model displays a range of behaviours unique to multidimensional systems while maintaining an ease of visualisation.

Hysteresis has been established as a key feature of complex Earth systems and their conceptual ecosystem counterparts (Dyke, 2008). Figure 6a shows a typical two environmental variable model which produces a number of homeostatic fixed points. The expected density of homeostatic model fixed points is Gaussian distributed,

$$n_0 = \exp\left(-\frac{P^\top P}{2}\right)\left(\frac{1}{\pi}\sqrt{\frac{1}{2\sigma_E^2}}\right)^N, \qquad (12)$$

and shown by Fig. 7 for a single environmental variable.

Applying increasing perturbing forces alters the attractor landscape, illustrated by Fig. 6 until the perturbation overcomes the regulatory ability of a fixed point, and a system occupying that point undergoes an abrupt transition. In many respects, it is appreciated that these simple hysteresis loops which occur in systems of one control dimension are a useful allegory for the behaviour of very much more complicated systems, of which almost all real systems may be considered an example. However there is a relative paucity of research which extends such iconic phenomena to more complicated, high dimensional systems. Figure 8 illustrates the complications which emerge from an increase to just two environmental dimensions; along with hysteresis loops, where the previous states of the system can be recovered either directly, or by steps through intermediate stable states, transitions exist where the previous state cannot be recovered simply by varying one perturbation dimension. Such states may require other forcing dimensions to be controlled, or much shorter time scale control such as shocks. As with the number of stable points in the essential range, the density of transitions with changes to perturbation can also be calculated, shown in Fig. 7.

Along with key questions surrounding the stationary behaviour of Earth-system models, we explore the nature of critical transitions or regime shifts, where small changes to an external forcing causes a dramatic change in the system state due to internal mechanisms (Williams and Lenton, 2010). Our model is suited to explore these phenomena as even one dimensional environments produce a range of stable states and external forcing terms can be added to produce abrupt transitions between them. Higher dimensional environments are shown to hold exponentially many such points and develop a diversity of intriguing dynamics such as a cusp bifurcation shown in Figs. 9 and 10 which emerge from the interactions between our diverse biota and an environment of at least two dimensions. These phenomena highlight the importance of understanding the major dimensions of control in a complex system as they describe a situation where one controlled variable changes the nature of a transition encountered by changes in another. Figure 9 shows that changes in perturbing force P_2 cause changes in the state of the environmental variable E_1, though these changes can be smooth or discontinuous depending on the value of another perturbing effect P_1. The phenomena has emerged simply from a randomly parametrised two dimensional model, and a thorough analysis proves this, along with the full spectrum of model behaviour, to be a result of our central assumptions of Sect. 3 rather than a specific implementation or parametrisation. This highlights the types of structures and attractors we expect from more complicated models and complex Earth systems.

5 Early warnings in complex ecosystems

Much of the work on early warning signals (EWS) has been carried out on simple models with limited behaviour and a small number of stable states (Held and Kleinen, 2004; van Nes and Scheffer, 2007; Guttal and Jayaprakash, 2008). As with these previous studies, we can show that our model is susceptible to early warning signal techniques while displaying the diverse phenomenology discussed in the previous section. There is a field of potential methods including analysis of signal autocorrelation and variance, associated with the phenomena of critical slowing down (CSD), along with skewness and flickering (Guttal and Jayaprakash, 2008; Brock and Carpenter, 2010). We study the variance, skewness and the autocorrelation or its inverse, the recovery rate, of our system when perturbed from its fixed point by stochastic forcing.

It should be noted that model fixed points are not consistent with the potential well illustrations of Scheffer et al. (2001); an N environmental variable system cannot be described by an N dimensional potential (the vector field $F(E)$ is not conservative except in models with a single environmental dimension, $N = 1$). Therefore it is not trivial to assume our model shares the EWS which emerge from such a mechanism.

Figure 10 illustrates the decay time of the system shown in Fig. 9 computed from the eigenvalues of the Jacobian of the system at the fixed points. Negative eigenvalues indicate that fixed points are stable, but additionally the inverse of the magnitude of eigenvalues provides us an estimate of the decay time of small fluctuations from the fixed point. Small negative eigenvalues correspond to a long decay time, indicating the system is in some sense slow, and recovery from small perturbations takes a long time. The convergence of eigenvalues, and therefore diverging decay time as a system approaches a critical transition is referred to as CSD (Critical Slowing Down) and it is postulated that this phenomena can be detected by observing either increasing signal variance or autocorrelation. However it appears to posses no further information pertaining to the direction, magnitude or reversibility of the transition; clearly important and relevant questions when considering transitions in real systems such as those seen in lake ecosystems and coral reefs where the conditions required for charophyte vegetation or widespread coral are not trivially restored following their collapse (Scheffer et al., 2001; Mumby et al., 2007). Figure 10a shows that in both directions, the decay time spikes at the transition and we therefore expect to be able to pick out a CSD signal in this type of system. Figure 10b also shows the decay time to become large, though strictly not divergent close to the point where the transition would occur for negative P_1. In a sense, this can be seen as misleading; in a real system, an investigator may expect an abrupt transition to some significantly different environmental state and may even measure false-positives for early warning signals, certainly for CSD, although in reality find a rapid but smooth and reversible variation.

In addition to these CSD EWS, the skewness of a signal has been put forward as an alternative. A signal becomes skewed when fluctuations about the mean are asymmetrical; perturbations in one direction elicit a different response to those in another direction. While the CSD techniques are based on the Jacobian, the first derivative of the dynamics, skewness is a measure of the second derivative. The derivation of Fig. 7 has proven the second derivative $\boldsymbol{F}''$ to be correlated with $\boldsymbol{F}$, leading to an increased tendency to encounter local extrema (where transitions occur) at large magnitude perturbations. We therefore expect, on average, to detect increased skewness where transitions are more likely, although not exclusively and without favour for a certain direction (positive or negative skewness).

We consider the application of these three techniques to a simulated data set, beginning by generating a time series from a stochastically increasing perturbation, $\boldsymbol{P}(t)$. Up to this point, the difference between time scales of changes in the biota, environment and perturbing force have been large. In order to relax the separation of biotic and environmental time scales, we use the homeostatic properties of the model to assume that changes in the state of the environmental variables is sufficiently slow that departures of the biota from its stationary value is small. In such a case, Eq. (9) is approximated by Newtonian relaxation into its stationary solution.

$$\tau_\alpha \frac{\mathrm{d}\boldsymbol{\alpha}(t)}{\mathrm{d}t} = \boldsymbol{\alpha}^*(\boldsymbol{E},\boldsymbol{\mu}) - \boldsymbol{\alpha}(t). \tag{13}$$

Previous work has shown that the relationship between the time scales of changes in the biota and changes in external perturbation set limits on the ability of other homeostatic systems to self-regulate; an unresponsive biota is unable to oppose changing perturbations and the regulatory system ultimately collapses (Weaver and Dyke, 2012). The perturbation is therefore chosen to increase over much longer time scales than the biotic response, and is chosen to follow a Weiner process where subsequent measurements are separated by small Gaussian distributed random numbers;

$$\left(P_1(t) - P_1(t+\Delta t)\right) \sim \mathcal{N}(\mu\Delta t, \sigma^2\Delta t) \tag{14}$$

where μ and σ^2 are the expected rate of increase in perturbing force and the variance of the increasing signal respectively. The perturbation drives the system through the transition shown in Fig. 10a. Estimations of the decay time of fluctuations within this time series may be found from the autocorrelation coefficient, exactly as Dakos et al. (2008).

The time series of Fig. 11a shows a two dimensional model with a stochastically increasing forcing term in one environmental dimension. Figure 10a analyses the Jacobian at the fixed points as this trajectory approaches a fixed point; as a stable fixed point becomes unstable, eigenvalues change sign and therefore at a transition, the leading eigenvalue approaches zero. This causes the decay time, that is the roughly exponential decay rate of small perturbations to the fixed point, diverges and the response of the system close to a perturbation is therefore expected to be slow, a recently popular suggestion for the behaviour of real Earth-systems in the vicinity of a critical transition (Lenton, 2011). Figure 11b verifies this for the stochastically driven model by showing significant increases in the autocorrelation coefficient of a simulated time series, quantified by the Kendall coefficient $\tau_K = 0.63$, indicating a positive trend with near certainty and corresponding to a strongly increasing decay time. Figure 11c shows the corresponding signal variance and yields a nearly monotonic increase indicated by $\tau_K = 0.99$ in contrast to Fig. 11d which, while showing a significant shift in the signed value of the skewness as the system approaches a transition, there is no such trend in the magnitude of the skewness, yielding $\tau_K = 0.41$ and -0.05 respectively, a result mirroring previous work which finds sign changes to obfuscate trends in the vicinity of transitions (Guttal and Jayaprakash, 2008). Furthermore, from Scheffer et al.'s (2001) potential well illustration, an increase in skewness is expected in the direction of the coming transition although we find this is not the case. Additional investigation of other model realizations and transitions reveals these EWS properties to be characteristic of the model, and the measured dimension to be unimportant.

While in this result, the presence of CSD is clear, we have generated data from a simulation and are free to vary parameters to our convenience. In reality, we may be further limited by the resolution of our time series, $1/\Delta t$, and the time scale of changes in the system compared to fluctuations, τ_α/τ_P. Figure 12 shows how the signal shown in Fig. 11b is improved or degraded by changes in these parameters, quantified by the Kendall rank coefficient. Measuring a significant signal requires that

1. the system responds sufficiently quickly to changes in perturbing forces that fluctuations are visible in the time series,
2. the interval between data points is sufficiently small compared to the time scale of changes to the biota that the relaxation can be resolved to some extent.

6 Discussion

The industrial revolution has granted humans an unprecedented level of influence over Earth system processes. The response of such processes to anthropogenic impacts is driving multiple challenges at varying scales. Climatic and ecosystem transitions threaten effects ranging from local extinctions to climate change and massive global biodiversity losses (Barnosky et al., 2012). Such transitions can have profound impacts on human society; newly realized states may not be so amenable to humans and pathways to revert to a previous state may be difficult (if not impossible) to traverse, particularly when critical transitions threaten to move the Earth system outside of any safe operating space for humanity (Rockstrom, 2009). There is urgent need to develop methods to anticipate critical transitions from empirical observations and evaluate their impact in order to make preparations and mitigate negative effects, or even avoid them entirely.

A number of studies have demonstrated the utility of autocorrelation, variance and skewness as indicators of impending critical transitions. Here, we demonstrated critical transitions in a model system that were a result of the interactions between the biota and environmental variables. An alternative perspective is that such interactions produce self-regulating or homeostatic states that are resilient to a range of perturbations. It is when this resilience fails that a critical transition is generated. We derived the density of transitions encountered by increases or decreases in perturbing forces. Transitions occur at local extrema of the effects of the model biota in the space of environmental variables. Such points indicate where there can be no further increase in the effect of the biota to offset further increases in external forcing, and thus the model undergoes a transition.

By examining our model, we see the leading eigenvalue of the system Jacobian converges in the vicinity of transitions, a property mirrored by a number of mathematical ecology models and consistent with CSD EWS (Held and Kleinen, 2004; van Nes and Scheffer, 2007). This is a result of transitions occurring at local extrema in the biotic effect function where the gradient approaches zero. Here, eigenvalues tend towards zero, and the decay time of small fluctuations from the fixed point diverge. This can, in theory, be detected from time series data by examining the signal variance or autocorrelation, AR(1), coefficient. Time series skewness is another contending EWS (Guttal and Jayaprakash, 2008); it has been shown that ecosystem dynamics have increased asymmetry in the vicinity of transitions, a property which may be measured from the second derivative of the model dynamics. All three EWS, the variance, autocorrelation and skewness show a strong trend as the model approaches a critical transition point, only the latter is ambiguous; while the signed value shows a strong trend from negative to positive, its magnitude does not and there is no reason for us to favour positive or negative skewness as a transition indicator.

Our model formulation allowed us to explore the consequences of explicitly including ecological dynamics into the simple models that form the theoretical foundation of early warning signal techniques. In particular, we went beyond a simple one dimensional representation of ecosystems and included a number of environmental processes that interacted directly and indirectly via a diverse community of individuals. While it would be expected that such an increase in model complexity would produce more complex dynamics, it is important to note that this led to a wide range both in the magnitude of critical transition between multiple stable states and degree of reversibility. We found that an examination of a range of early warning signals conveyed no further information about the magnitude or reversibility of a critical transition. In that respect, the difference between a reliable early warning signal and a type 1 error or false positive may be moot. Given there is no correlation between the significance of the early warning signal and the magnitude and/or reversibility of the critical transition, situations arise where early warning signals are given for transitions that are both trivial to reverse and effectively impossible to recover from. The implications of this finding are important for environmental management. For example, attempts to recover fresh water lakes from eutrophic conditions as a consequence of excessive phosphorus input by reducing future phosphorus inputs may be misguided; while the critical transition was initiated by excessive phosphorus input, reducing such inputs will not lead to reversal in water phosphorus concentration as a powerful feedback loop involving both biotic and abiotic processes has been initiated (Conley et al., 2009). Considering such critical transitions in the light of social-ecological dynamics introduces more model complexity (Zhang et al., 2015).

7 Conclusions

The model presented in this paper demonstrates the emergence of critical transitions between multiple ecological stable states. These dynamics were the result of a diverse biota interacting with environmental processes. The conceptual formulation of the model allowed an in-depth analysis, and we determined the density of stable states and critical transitions along with the occurrence of early warning signals. Prior to transitions the model exhibited critical slowing down, evidenced by increases in the autocorrelation and variance of time series data, along with changes in signal skewness. These measures have been proposed as robust indicators of critical transitions in real-world systems. We show that while the signals can be reliably produced, the amount of information conveyed about the future state of the system is limited. In particular, given a system with multiple stable states and more than one environmental variable, it was

Title Page
Abstract | Introduction
Conclusions | References
Tables | Figures
◀| |▶
◀ ▶
Back | Close
Full Screen / Esc
Printer-friendly Version
Interactive Discussion

found that no proposed early warning signal indicates the size or reversibility of the proximate critical transition. We presented results in which a critical transition produced by a particular driving force on a particular environmental variable cannot be reversed by altering the sign of that driving force. Given that real-world systems are likely to be significantly more complex than our conceptual model formulation, we conclude that it is necessary to understand the underlying dynamics and processes of such real-world systems in order to contextualise any early warning signal.

Acknowledgements. This work was supported by a University of Southampton EPSRC Doctoral Training Partnership 2014 grant (EP/M50662X/1).

References

Barnosky, A. D., Hadly, E. A., Bascompte, J., Berlow, E. L., Brown, J. H., Fortelius, M., Getz, W. M., Harte, J., Hastings, A., Marquet, P. A., Martinez, N. D., Mooers, A., Roopnarine, P., Vermeij, G., Williams, J. W., Gillespie, R., Kitzes, J., Marshall, C., Matzke, N., Mindell, D. P., Revilla, E., and Smith, A. B.: Approaching a state shift in Earth's biosphere, Nature, 486, 52–58, doi:10.1038/nature11018, 2012. 2524

Brock, W. A. and Carpenter, S. R.: Interacting regime shifts in ecosystems: implication for early warnings, Ecol. Monogr., 80, 353–367, doi:10.1890/09-1824.1, 2010. 2520

Carpenter, S. R.: Eutrophication of aquatic ecosystems: bistability and soil phosphorus, P. Natl. Acad. Sci. USA, 102, 10002–10005, doi:10.1073/pnas.0503959102, 2005. 2511

Carpenter, S. R. and Brock, W. A.: Rising variance: a leading indicator of ecological transition, Ecol. Lett., 9, 311–318, doi:10.1111/j.1461-0248.2005.00877.x, 2006. 2510

Carpenter, S. R., Ludwig, D., and Brock, W. A.: Management of eutrophication for lakes subject to potentially irreversible change, Ecol. Appl., 9, 751–771, doi:10.1890/1051-0761(1999)009[0751:MOEFLS]2.0.CO;2, 1999. 2508, 2511

Carpenter, S. R., Cole, J. J., Pace, M. L., Batt, R., Brock, W. A., Cline, T., Coloso, J., Hodgson, J. R., Kitchell, J. F., Seekell, D. A., Smith, L., and Weidel, B.: Early warnings of regime shifts: a whole-ecosystem experiment, Science, 332, 1079–1082, doi:10.1126/science.1203672, 2011. 2511

Conley, D. J., Paerl, H. W., Howarth, R. W., Boesch, D. F., Seitzinger, S. P., Havens, K. E., Lancelot, C., and Likens, G. E.: ECOLOGY: controlling eutrophication: nitrogen and phosphorus, Science, 323, 1014–1015, doi:10.1126/science.1167755, 2009. 2526

Dakos, V., Scheffer, M., van Nes, E. H., Brovkin, V., Petoukhov, V., and Held, H.: Slowing down as an early warning signal for abrupt climate change, P. Natl. Acad. Sci. USA, 105, 14308–14312, doi:10.1073/pnas.0802430105, 2008. 2509, 2523

Dyke, J. G.: Entropy Production in an Energy Balance Daisyworld Model, Artificial Life, MIT Press, Cambridge, MA, 2008. 2519

Dyke, J. G. and Weaver, I. S.: The emergence of environmental homeostasis in complex ecosystems, PLoS Comput. Biol., 9, e1003050, doi:10.1371/journal.pcbi.1003050, 2013. 2509, 2512, 2513, 2516, 2518, 2537

Goldblatt, C., Lenton, T. M., and Watson, A. J.: Bistability of atmospheric oxygen and the great oxidation, Nature, 443, 683–686, doi:10.1038/nature05169, 2006. 2514

Guttal, V. and Jayaprakash, C.: Changing skewness: an early warning signal of regime shifts in ecosystems, Ecol. Lett., 11, 450–460, doi:10.1111/j.1461-0248.2008.01160.x, 2008. 2510, 2520, 2523, 2525

Held, H. and Kleinen, T.: Detection of climate system bifurcations by degenerate fingerprinting, Geophys. Res. Lett., 31, L23207, doi:10.1029/2004GL020972, 2004. 2520, 2525

Jones, C. G., Lawton, J. H., and Shachak, M.: Organisms as ecosystem engineers, Oikos, 69, 373–386, 1994. 2514

Kleinen, T., Held, H., and Petschel-Held, G.: The potential role of spectral properties in detecting thresholds in the Earth system: application to the thermohaline circulation, Ocean Dynam., 53, 53–63, doi:10.1007/s10236-002-0023-6, 2003. 2510

Lenton, T. M.: Early warning of climate tipping points, Nature Climate Change, 1, 201–209, doi:10.1038/nclimate1143, 2011. 2509, 2511, 2523

Lenton, T. M., Held, H., Kriegler, E., Hall, J. W., Lucht, W., Rahmstorf, S., and Schellnhuber, H. J.: Tipping elements in the Earth's climate system, P. Natl. Acad. Sci. USA, 105, 1786–1793, doi:10.1073/pnas.0705414105, 2008. 2508

Lenton, T. M., Livina, V. N., Dakos, V., van Nes, E. H., and Scheffer, M.: Early warning of climate tipping points from critical slowing down: comparing methods to improve robustness, Philos. T. R. Soc. A, 370, 1185–1204, doi:10.1098/rsta.2011.0304, 2012. 2508

Lu, Z.: Global stability for a Lotka-Volterra system with a weakly diagonally dominant matrix, Appl. Math. Lett., 11, 81–84, doi:10.1016/S0893-9659(98)00015-9, 1998. 2516

May, R. M., Levin, S. A., and Sugihara, G.: Complex systems: ecology for bankers, Nature, 451, 893–895, doi:10.1038/451893a, 2008. 2508, 2510

Mumby, P. J., Hastings, A., and Edwards, H. J.: Thresholds and the resilience of Caribbean coral reefs, Nature, 450, 98–101, doi:10.1038/nature06252, 2007. 2521

Odling-Smee, F. J., Laland, K. N., and Feldman, M.: Niche Construction: The Neglected Process in Evolution, Princeton University Press, Princeton, 2003. 2514

Rockstrom, J. E. A.: A safe operating space for humanity, Nature, 461, 472–475, doi:10.1038/461472a, 2009. 2524

Sanders, D. and van Veen, F. J. F.: Ecosystem engineering and predation: the multi-trophic impact of two ant species, J. Anim. Ecol., 80, 569–576, doi:10.1111/j.1365-2656.2010.01796.x, 2011. 2514

Scheffer, M., Carpenter, S. R., Foley, J. A., Folke, C., and Walker, B.: Catastrophic shifts in ecosystems, Nature, 413, 591–596, doi:10.1038/35098000, 2001. 2508, 2510, 2521, 2523

Scheffer, M., Bascompte, J., Brock, W. A., Brovkin, V., Carpenter, S. R., Dakos, V., Held, H., van Nes, E. H., Rietkerk, M., and Sugihara, G.: Early-warning signals for critical transitions, Nature, 461, 53–59, doi:10.1038/nature08227, 2009. 2508, 2509, 2511

Scheffer, M., Carpenter, S. R., Dakos, V., and van Nes, E.: Generic indicators of ecological resilience, Annu. Rev. Ecol. Evol. S., 46, doi:10.1146/annurev-ecolsys-112414-054242, 2015. 2509

Sornette, D.: Predictability of catastrophic events: material rupture, earthquakes, turbulence, financial crashes, and human birth, P. Natl. Acad. Sci. USA, 99 Suppl 1, 2522–2529, doi:10.1073/pnas.022581999, 2002. 2511

Tyrrell, T.: Biotic plunder: control of the environment by biological exhaustion of resources, in: Scientists Debate Gaia: The Next Century, MIT Press, Cambridge, MA, 137–147, 2004. 2511

van Nes, E. H. and Scheffer, M.: Slow recovery from perturbations as a generic indicator of a nearby catastrophic shift, Am. Nat., 169, 738–747, doi:10.1086/516845, 2007. 2520, 2525

van Nes, E. H., Holmgren, M., Hirota, M., and Scheffer, M.: Response to Comment on “Global resilience of tropical forest and savanna to critical transitions”, Science, 336, 541 pp., doi:10.1126/science.1219711, 2012. 2508

Venegas, J. G., Winkler, T., Musch, G., Vidal Melo, M. F., Layfield, D., Tgavalekos, N., Fischman, A. J., Callahan, R. J., Bellani, G., and Harris, R. S.: Self-organized patchiness in asthma as a prelude to catastrophic shifts, Nature, 434, 777–782, doi:10.1542/peds.2006-0900SS, 2005. 2510

Weaver, I. S. and Dyke, J. G.: The importance of timescales for the emergence of environmental self-regulation, J. Theor. Biol., 313, 172–180, doi:10.1016/j.jtbi.2012.07.034, 2012. 2512, 2522

Weaver, I. S. and Dyke, J. G.: Tipping points in complex coupled life-environment systems, in: Advances in Artificial Life, ECAL 2013, MIT Press, Cambridge, MA, 387–394, doi:10.7551/978-0-262-31709-2-ch056, 2013. 2512, 2515

Wilkinson, M. T., Richards, P. J., and Humphreys, G. S.: Breaking ground: pedological, geological, and ecological implications of soil bioturbation, Earth-Sci. Rev., 97, 257–272, doi:10.1016/j.earscirev.2009.09.005, 2009. 2514

Williams, H. T. P. and Lenton, T. M.: Evolutionary regime shifts in simulated ecosystems, Oikos, 119, 1887–1899, doi:10.1111/j.1600-0706.2010.18127.x, 2010. 2519

Zeeman, E. C.: Catastrophe theory, in: Structural Stability in Physics, chap. Catastroph, Springer, Berlin, doi:10.1007/978-3-642-96937-9, 1976. 2508

Zhang, K., Dearing, J. A., Dawson, T. P., Dong, X., Yang, X., and Zhang, W.: Poverty alleviation strategies in eastern China lead to critical ecological dynamics, Sci. Total Environ., 506–507, 164–181, doi:10.1016/j.scitotenv.2014.10.096, 2015. 2526

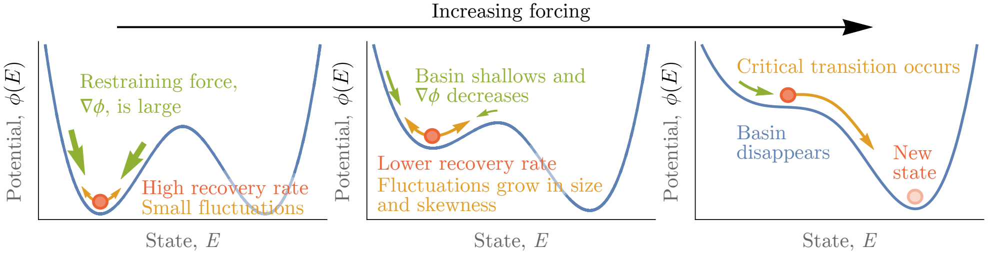

Figure 1. A simple mechanism which produces a CSD signal is the above potential with two stable points, indicated by the minima of the two basins. Initially, the potential is steep and fluctuations about the stable state are strongly reigned back. As forcing increases, the basin the system occupies degrades, becoming shallower and the forces correspondingly weaker, leading to slower, and larger fluctuations. Eventually the basin is completely eroded and a critical transition occurs to the remaining stable state.

Title Page
Abstract | Introduction
Conclusions | References
Tables | Figures
◀| |▶
◀ ▶
Back | Close
Full Screen / Esc
Printer-friendly Version
Interactive Discussion

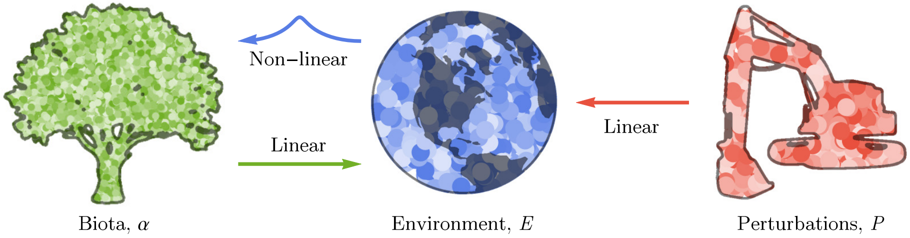

Figure 2. The model biota consists of a large number, K, elements in the vector $\boldsymbol{\alpha}$. They are linearly coupled to their N environmental variables in vector $\boldsymbol{E}$ by the random, zero-mean coupling coefficients $\boldsymbol{\Omega}$. In turn, the environment determines their individual abundance by a simple niche idea; biotic elements are maximally abundant in the vicinity of their niche, $\boldsymbol{\mu}$. The environment is also subject to a linear forcing term $\boldsymbol{P}$.

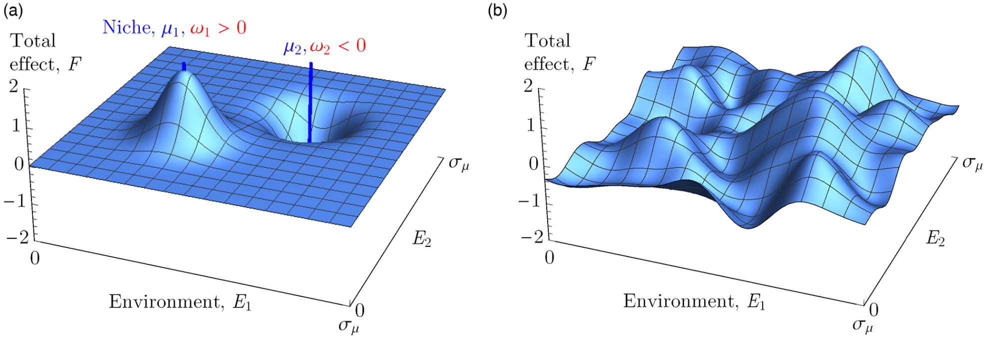

Figure 3. $K = 2$ biotic elements with an increasing ($\omega_1 > 0$) and decreasing ($\omega_2 < 0$) effect on one environment variable are illustrated by **(a)** along with their niche positions. As K becomes large, the essential range is populated by a diverse biota and the net effect maintains zero mean, but significant variance, illustrated by **(b)**.

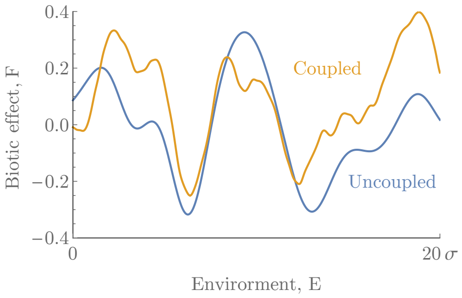

Figure 4. The summed effect of the biota F is shown for model parameters $K = 100$, $\sigma_E = \frac{1}{20}\sigma_\mu$. The addition of biotic coupling via the competitive Lotka-Volterra equation does not change the central behaviour of the model. Furthermore, the characteristic scale of the total effect function with changes in E is largely unchanged.

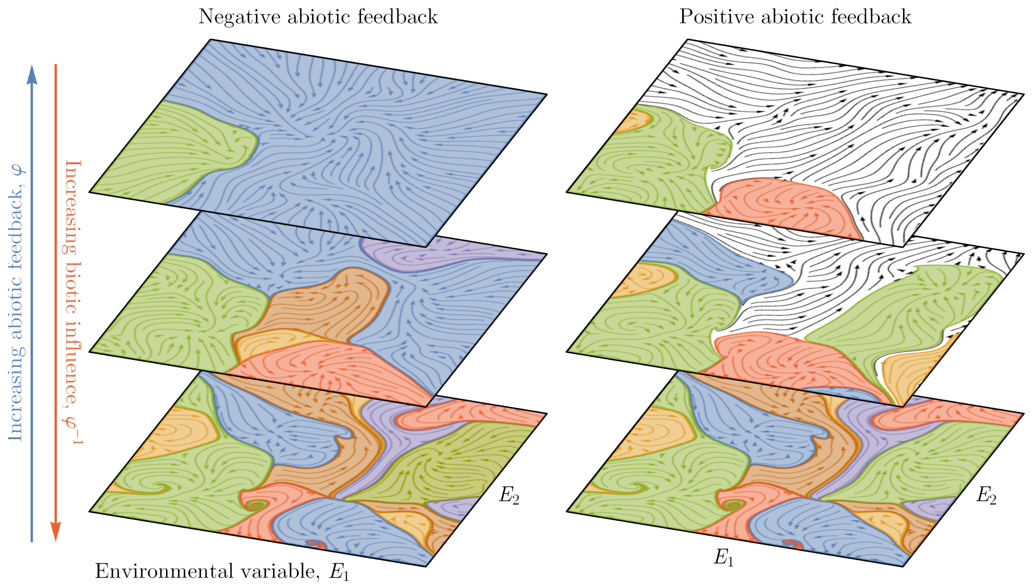

Figure 5. The flow of a two environmental variable model is shown for attractive and repulsive environmental fixed points with a range of strengths. Increasing environmental feedback decreases the density of fixed points. In the case of attractive abiotic fixed points, this leads to larger portions of the environment being absorbed into the abiotic fixed point. Increasing the repulsive abiotic feedback however ejects larger portions of the environmental variable space from the essential range, indicated in white.

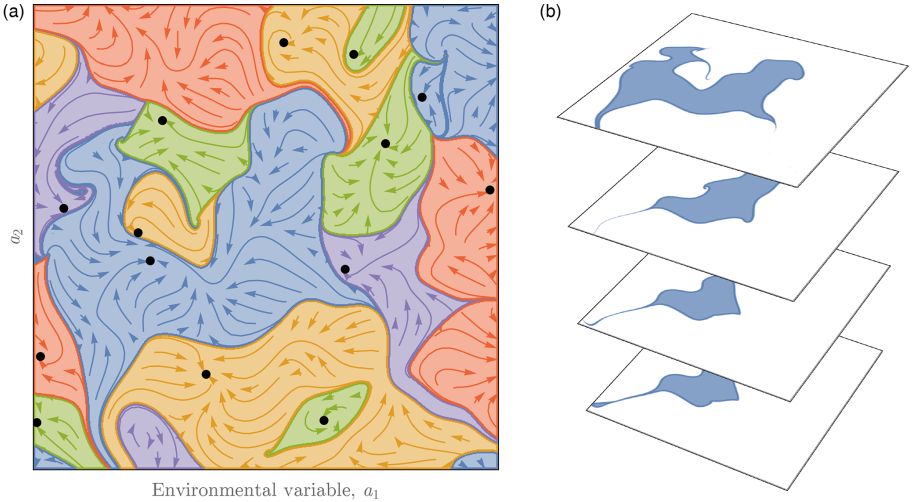

Figure 6. At a particular value for the external perturbing force ***P***, the model has a number of fixed points, shown in **(a)** along with their basin of attraction in a two dimensional environment. As the perturbing force changes, **(b)** shows the warping of one such basins which would eventually disappear entirely, corresponding to a model transition from one fixed point to another.

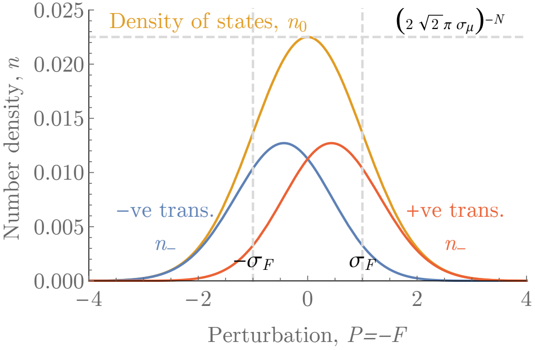

Figure 7. The density of stable fixed points in the model is determined only by the characteristic width of the biotic niche functions and the magnitude of external perturbation (Dyke and Weaver, 2013). Providing the size of the biota K is large such that the total effect of the biota is well approximated by a Gaussian process, the specific form of niche function and biotic diversity is unimportant. The corresponding transition density, the expected number of model transitions encountered by increasing, n_+ and decreasing, n_- perturbation magnitude, shows that a model exposed to an increasing perturbation is also more and increasingly likely to undergo a transition due to further increases in the perturbation than decreases, and vice-versa.

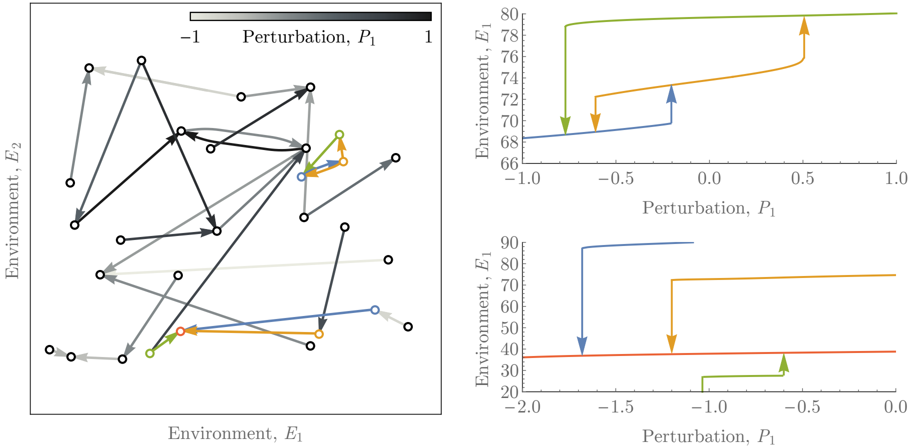

Figure 8. A network emerges between the model fixed points as perturbing forces vary, illustrated by **(a)**. Black circles indicate homeostatic fixed points, while arrows show transitions which occur between them for a $N = 2$ environmental variable model, driven by a single forcing term in one environmental dimension. Both the stable points and transitions emerge with predictable density, given by Fig. 7. Some transitions may be reversed either directly, or though intermediate states, by varying the forcing term in the opposite direction to that which caused the transition. This causes hysteresis, such as between homeostatic states shown by **(b)**. Others cannot; having undergone a transition to certain states, the system cannot recover its previous state by varying this forcing dimension.

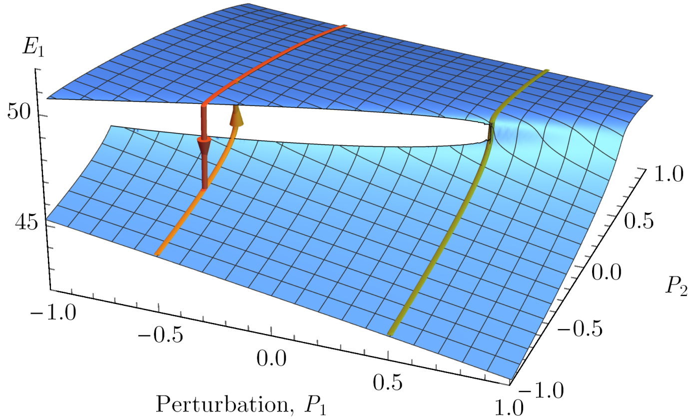

Figure 9. Two stable states which emerge from a $N = 2$ environmental variable system. The surface shows the environmental state is approximately constant with changes in perturbing forces P_1 and P_2. While these fixed points are homeostatic and stable in the face of forcing in both environmental variables, there is a hysteretic shift within the attractor when the perturbation P_1 is negative, detailed in **(a)**, in contrast to positive perturbations which find continuous variation shown in **(b)**. This is commonly referred to as a cusp bifurcation, where the qualitative nature of a transition caused by changes in one variable is dependant on another, and has emerged simply as a consequence of the assumptions of Sect. 3.

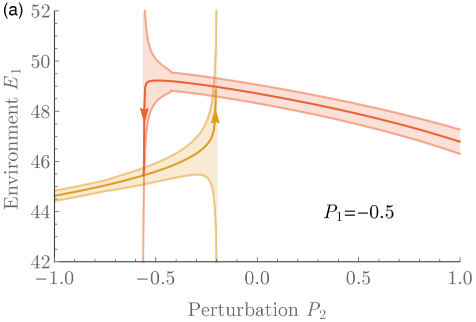

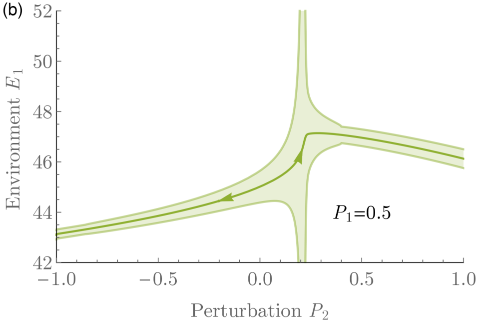

Figure 10. Two cross-sections of Fig. 9 showing that the state of perturbation P_1 dictates the type of transition encountered by changes in P_2. The shaded region indicates the lifetime of fluctuations in the steady state which diverge as the system approaches a critical transition. **(a)** shows a discontinuous transition caused by changes in P_2 where P_1 is positive while a smooth transition caused by changes in P_2 where P_1 is negative, illustrated by **(b)**.

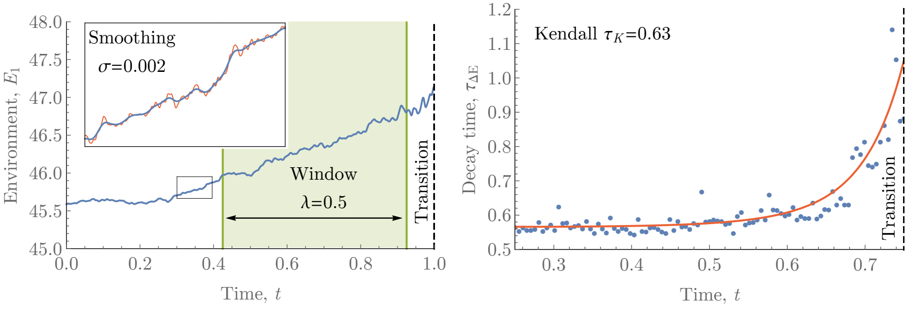

(a) A transition caused by stochastically increasing forcing.

(b) Decay time is calculated from the AR(1) coefficients.

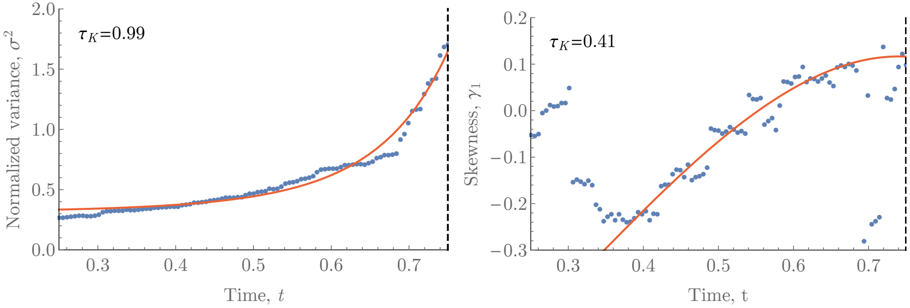

(c) Signal variance.

(d) Signal skewness.

Figure 11. The same transition encountered by increasing perturbation in the positive direction in Fig. 10a is simulated with stochastically increasing forcing, modelled by a positive biased Wigner process, generating the time series shown by **(a)**. An autoregression process $E(t+1) = E(t)\alpha + \epsilon(t)$ is fit to a sliding window of time series data, λ, and the decay time of small perturbation from the stationary points can be estimated by the AR(1) coefficient shown in **(b)**. Similarly, we measure the signal variance and skewness in the sliding window, shown in **(c, d)** respectively. The increasing trend in the autocorrelation, variance and skewness are quantified by Kendall coefficients of 0.67, 0.99 and 0.41 respectively.

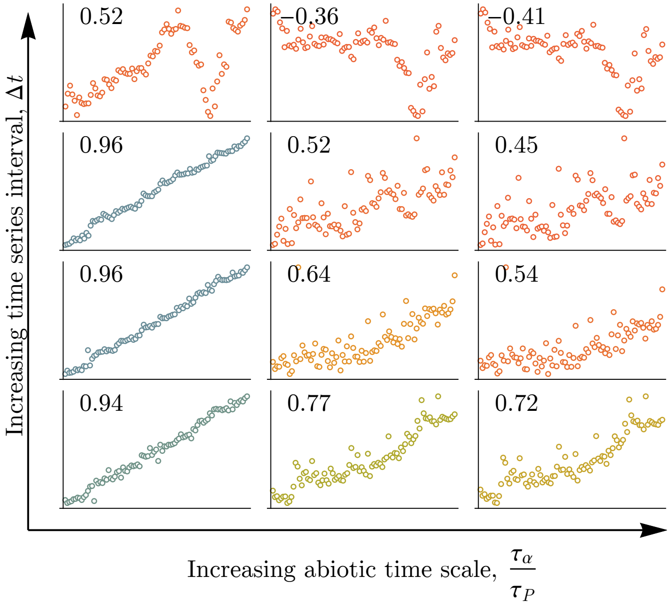

Figure 12. The strength of the CSD signal shown by Fig. 11 and as measured by the Kendall coefficient, is sensitive to the relative time scales both of the response of the composition of the biota to changes in their environment, and the measurements which make up the time series data. Clearly we require that the biota responds sufficiently quickly that it is both measurable and present in the dynamics, while also requiring that our data points are sufficiently dense to resolve the relaxation of the system towards its fixed point.